Apoptosis (2010) 15:474–487
DOI 10.1007/s10495-009-0438-3

ORIGINAL PAPER

AChE deficiency or inhibition decreases apoptosis and p53 expression and protects renal function after ischemia/reperfusion

Weiyuan Ye · Xiaowen Gong · Jing Xie · Jun Wu · Xuejin Zhang · Qi Ouyang · Xiaolin Zhao · Yufang Shi · Xuejun Zhang

Published online: 7 January 2010

Abstract We recently reported that the expression of the synaptic form of acetylcholinesterase (AChE) is induced during apoptosis in various cell types in vitro. Here, we provide evidence to confirm that AChE is expressed during ischemia–reperfusion (I/R)-induced apoptosis in vivo. Renal I/R is a major cause of acute renal failure (ARF), resulting in injury and the eventual death of renal cells due to a combination of apoptosis and necrosis. Using AChE-deficient mice and AChE inhibitors, we investigated whether AChE deficiency or inhibition can protect against apoptosis caused by I/R in a murine kidney model. Unilateral clamping of renal pedicles for 90 min followed by reperfusion for 24 h caused significant renal dysfunction and injury. Both genetic AChE deficiency and chemical inhibition of AChE (provided by huperzine A, tacrine and donepezil) significantly reduced the biochemical and histological evidence of renal dysfunction following I/R. Activation of caspases-8, -9, -12, and -3 in vivo were prevented and associated with reduced levels of cell apoptosis and cell death. A further investigation also confirmed that AChE deficiency down-regulated p53 induction and phosphorylation at serine-15, and decreased the Bax/Bcl-2 ratio during I/R. In conclusion, our study demonstrates that AChE may be a pro-apoptotic factor and the inhibition of AChE reduces renal I/R injury. These findings suggest that AChE inhibitors may represent a therapeutic strategy for protection against ischemic acute renal failure.

Keywords Apoptosis · Acetylcholinesterase · Acetylcholinesterase inhibitors · Ischemia/reperfusion

Abbreviations

AChE	Acetylcholinesterase
AChEIs	Acetylcholinesterase inhibitors
AD	Alzheimer's disease
ARF	Acute renal failure
GSK 3	Glycogen synthase kinase 3
I/R	Ischemia-reperfusion
JNK	The c-Jun-N-terminal kinase

Weiyuan Ye and Xiaowen Gong have contributed equally to this article.

W. Ye · X. Gong · J. Xie · J. Wu · X. Zhang · Q. Ouyang · X. Zhao · X. Zhang (✉)
Laboratory of Molecular Cell Biology, Institute of Biochemistry and Cell Biology, Shanghai Institutes for Biological Sciences, Graduate School of the Chinese Academy of Sciences, Chinese Academy of Sciences, 320 Yueyang Road, 200031 Shanghai, China
e-mail: xjzhang@sibs.ac.cn

W. Ye
e-mail: wyye@sibs.ac.cn

X. Gong
e-mail: xwgon@sibs.ac.cn

J. Xie
e-mail: jxie@sibs.ac.cn

X. Zhang
e-mail: zhangxuejin@sibs.ac.cn

Q. Ouyang
e-mail: ouyangqi823@sohu.com

X. Zhao
e-mail: xiao_lin_1985@hotmail.com

Y. Shi
Department of Molecular Genetics, Microbiology and Immunology, University of Medicine and Dentistry of New Jersey-Robert Wood Johnson Medical School, New Brunswick, NJ, USA
e-mail: shiyu@umdnj.edu

TUNEL Terminal deoxynucleotidyltransferase-mediated dUTP nick-end-labeling

Introduction

The classical role of acetylcholinesterase (AChE, EC 3.1.1.7) is to terminate cholinergic neurotransmission by rapid hydrolysis of the neurotransmitter acetylcholine (ACh) at cholinergic synapses and neuromuscular junctions [1]. In mammals, AChE is encoded by a single gene, *ache*, however, because of alternative splicing at the C-terminus of acetylcholinesterase mRNA, three different isoforms occur: AChE-S (synaptic isoform), AChE-E (erythtocytic isoform) and AChE-R (read-through isoform) [2]. We have reported that AChE-S expression was induced during apoptosis in various cell types including non-muscle, non-nervous and non-hematopoietic cell lines by different apoptotic stimuli, and the blockage of AChE expression by antisense RNA prevents the induction of apoptosis [3]. More recently, overexpression of an N-terminally extended AChE-S variant was shown to activate Tau kinase, GSK3 (glycogen synthase kinase 3), Tau hyper-phosphorylation, caspase-3 and cause apoptosis [4].

Cholinergic neurons are extensively implicated in cognitive functioning and Alzheimer's disease (AD) is a chronic neurodegenerative disorder characterized by a progressive loss of cholinergic neurons. Acetylcholinesterase inhibitors (AChEIs) may block the degradation of acetylcholine, thus increasing the efficacy of the remaining cholinergic neurons. However, most AChEIs also have the ability to protect cells against cell death induced by various apoptotic stimuli with different mechanisms of action [5–11]. All of these studies were based on cell lines derived from the central or peripheral nervous system, and the anti-apoptotic mechanisms involved down-regulation of pro-apoptotic p53 and bax, the stimulation of anti-apoptotic bcl-2 [5, 6],or the direct blocking of NMDA receptors [11]. Results from an in vivo model also demonstrated that bis(7)-tacrine, an AChEI, could protect against acute focal cerebral ischemic insults [12].

To examine whether AChE-S expression can be detected in non-nervous tissues during apoptosis in vivo, and to further investigate the role of AChE-S in this process, we established a murine renal I/R model to induce apoptosis. In this study, we found that that the expression of AChE-S was markedly increased in renal I/R induced tubule apoptosis. Utilizing AChE-deficient mice and three different AChE inhibitors including huperzine A, tacrine and donepezil, we demonstrated that both AChE deficiency and inhibition significantly reduced apoptosis induced by acute renal ischemic injury. Also, a further investigation confirmed that AChE deficiency attenuated I/R-induced over-expression of p53 and Bax and augmented the level of Bcl-2. Additionally, our results demonstrated that not only the 68 kDa AChE-S but also a 55/50 kDa isoform was detected in apoptotic cells.

Materials and methods

Animals

AChE knockout mice (stock number 005987) were purchased from the Jackson Laboratory. The $AChE^{+/+}$ and $AChE^{+/-}$ mice were used for experiments at 8 weeks of age. Male Sprague–Dawley rats (250–300 g) were purchased from the Shanghai Slac Laboratory Animal Co. Ltd. Animals were housed under standard conditions of light and dark cycle with free access to food and water. The experimental protocols were approved by the Institutional Animal Ethics Committee of the Shanghai Institutes for Biological Sciences.

Identification of AChE-deficient mice

AChE-deficient mice were identified by PCR analysis with specific genotyping protocols obtained from the Jackson Laboratory website.

Surgery and experimental protocols

The animals were anesthetized with sodium pentobarbital (55 mg/kg, ip.). A midline incision was made and both kidneys were isolated. The left renal pedicle was occluded by clamping the left renal artery for 90 min after right nephrectomy and then followed by 24 h reperfusion.

Mice were divided into the following groups, which consisted of four to six animals:

(1) Wild-type (WT) nephrectomized Sham group (WT Sham)
(2) WT nephrectomized I/R group (WT I/R)
(3) Heterozygous AChE deficiency nephrectomized Sham group (Heterozygous Sham)
(4) Heterozygous AChE deficiency nephrectomized I/R group (Heterozygous I/R)

Rats were divided into five groups each consisting of eight to ten animals.

(1) Saline-treated nephrectomized Sham group (Sham)
(2) Saline-treated nephrectomized I/R group (I/R)
(3) Huperzine A-treated nephrectomized I/R group (I/R+ Huperzine A), rats were administered ip. 0.25 mg/kg

huperzineA 4 times on the first day, then were injected with 0.125 mg/kg huperzine A 4 times on the second day, and the fifth injection of was 1 h prior to the right nephrectomy and I/R.

(4) Tacrine-treated nephrectomized I/R group (I/R+ Tacrine), rats were administered ip. 4.5 mg/kg tacrine 4 times on the first day, then were injected with 2.25 mg/kg tacrine 4 times on the second day, and the fifth injection was 1 h prior to the right nephrectomy and I/R.

(5) Donepezil-treated nephrectomized I/R group (I/R+ Donepezil), rats were administered ip. 6 mg/kg donepezil once daily for 4 days, then a fifth injection of 3.0 mg/kg donepezil was administered 1 h prior to surgery.

Sham-operated animals underwent identical surgical procedures but the left renal pedicle was not occluded. AChE is intensely expressed in the human central nervous system [1], megakaryocytes and erythrocytes [13, 14]. In order to attain efficient AChE inhibition homeostasis, AChE inhibitors were administered 4 times before the fifth injection, which was given 1 h prior to ischemia. Also, the dosing intervals are approximately equal to the half-life of the drugs. The injections after ischemic surgery are in the interest of inhibition of apoptosis induced AChE. After surgery, the animals were returned to the cages, where they had free access to food and water.

At the end of 24 h of reperfusion, the animals were sacrificed and blood was collected from the heart. Harvested kidney samples were kept in deep frozen condition for further analysis.

AChE immunofluorescence and TUNEL

AChE immunofluorescence and fluorescein labeled TUNEL double staining protocols have been previously described [3, 15]. A peroxidase labeled TUNEL In Situ Apoptosis Detection Kit (KeyGen Biotech., Nanjing, China) was also used according to the manufacturer's protocol. The nuclei were lightly counterstained with hematoxylin. For each paraffin section, at least 6–10 fields were randomly selected and the frequency of TUNEL-positive cells was estimated at ×400 magnification.

Histological examination

Paraformaldehyde-fixed (4%) and paraffin-embedded kidneys were sectioned at 3 μm and stained with hematoxylin-eosin using standard methods. Histological examinations were performed by the renal pathologist (M.S. Lucia) in a blinded fashion. Histological changes due to tubular necrosis were quantitated by counting the percent of tubules that displayed cell necrosis, loss of brush border, cast formation, and tubule dilatation as follows: 0 = none, 1 ≤ 10%, 2 = 11–25%, 3 = 26–45%, 4 = 46–75%, and 5 ≥ 76%. At least 6–10 fields (×200) were reviewed for each slide.

Assessment of renal function

Serum creatinine and blood urea nitrogen (BUN) levels were assayed in serum samples by hospital research services.

Western blot analysis

Immunoblotting protocols have been previously described [3, 15].

Anti-cleaved caspase-3 (9661#), anti-caspase-9 (9506#) and anti-p-p53 (9284#) antibodies were purchased from Cell Signaling. Anti-caspase-12 (3182#) antibody was supplied by Biovision. The anti-caspase-8 (sc-5263), anti-p53 (sc-6243), anti-Bax (sc-7480), anti-Bcl-2 (sc-7382) and anti-beta-actin antibodies were provided by Santa Cruz. The bands on the membranes were scanned and their densities were analyzed by Quantity One software.

Semiquantitative RT–PCR and real-time PCR

Total RNA was extracted from cells using TRIzol Reagent (Invitrogen) and was reverse transcribed using M-MLV Reverse Transcriptase (Promega). The resulting cDNAs were used as a template to amplify AChE-S via PCR (575 bp fragment; F, 5′-CGGGTCTATGCCTACATC-3′; R,5′-GCTCGGTCGTATTATATCCCA-3′), AChE-R (573 bp fragment; F, 5′-CCGGGTCTATGCCTACATCTTTGAA-3′; R,5′-AAGGAAGAAGAGGAGGGACAGGGCTAAG-3′), AChE-E (457 bp fragment; F, 5′-CCGGGTCTATGCCTACATCTTTGAA-3′; R,5′-AAGGAAGAAGAGGAGGGACAGGGCTAAG-3′), actin (257 bp fragment; F 5′-CAACTCCATCATGAAGTGTGACG-3′; R, 5′-ACTCGTCATACTCCTGCTTGC-3′).

Real-time PCR was performed using an ABI 7500 fast sequence detection system (Applied Biosystems) with SYBR green fluorescent label. Samples (10 μl final) contained the following: 1 × Power SYBR Green PCR Master Mix (Applied Biosystems), 3–5 pmol of each primer, and 0.25 μl of the RT reaction. Samples were run in triplicate in optically clear 384-well plates (Corning, NY). Cycling parameters were as follows: 95°C × 10 min, followed by 40 cycles of 95°C for 15 s, 60°C for 1 min, and a detection step at 72°C for 30 s. β-actin transcript was used in each sample as an internal reference to standardize the results by eliminating variations in mRNA and cDNA quantity and quality. Each RNA sample was run in triplicate with three

samples per exposure regime. A single peak in all dissociation curves verified production of a single amplicon per primer pair.

Determination of AChE activities

Relative AChE activities of the homogenate were determined spectrophotometrically in a 96-well plate using a modified Ellman's assay as described previously [16] and normalized against total protein.

Statistical analysis

The data are presented as means ± SE. Statistical analysis was performed using one-way ANOVA, followed by Newman–Keuls multiple comparisons. $P < 0.05$ was considered statistically significant.

Results

Identification of AChE knockout mice

AChE$^{+/-}$ animals were initially identified using PCR analysis (Fig. 1A). Western blot analysis confirmed that the level of AChE protein expression in renal tissues of $AChE^{+/-}$ mice was approximately half the level of AChE protein detected in $AChE^{+/+}$ mice, and AChE was not expressed in $AChE^{-/-}$ mice (Fig. 1B).

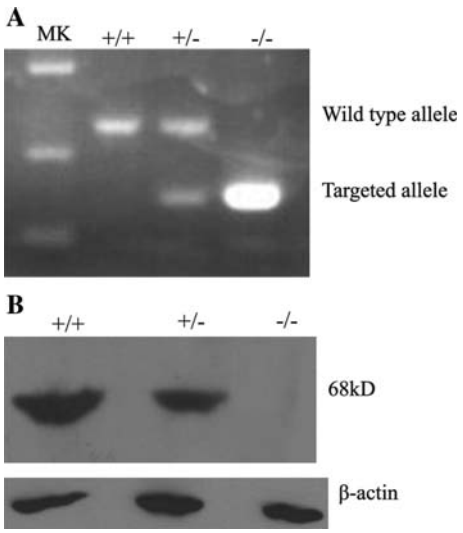

Fig. 1 Identification of AChE knockout mice. **A** PCR-based genotyping of WT and AChE-deficient mice. **B** Western blot analysis of AChE protein expression in normal renal tissues of WT and AChE-deficient mice

Induction of AChE expression during apoptosis triggered by acute renal I/R injury

In comparison with sham animals, renal I/R remarkably induced apoptosis. Apoptosis was assessed by a significant increase in activated caspase-3 (Fig. 2A). AChE-S expression during apoptosis induced by renal I/R was also investigated by RT–PCR and Western blot analysis using a monoclonal antibody against a specific C-terminal peptide derived from AChE-S [15], revealed that AChE-S was significantly increased both in mRNA and protein levels (Fig. 2B–D). To determine if a correlation between apoptosis and AChE expression existed, genomic DNA fragmentation was assayed by TUNEL staining and AChE protein expression was detected by immunofluorescence in renal tissue sections. Most of the apoptotic cells detected were positive for both genomic DNA fragmentation and AChE expression, while living cells were negative for both (Fig. 2E). Interestingly, in addition to the 68 kDa form of AChE-S, a 55/50 kDa isoform was found to have a positive correlation with apoptosis and was detected in apoptotic cells by Western blot analysis (Figs. 2D, 6).

AChE deficiency or inhibition attenuates the histomorphologic changes of I/R injury

The presence of apoptotic cells was confirmed by the detection of shrunken and condensed nuclei with hematoxylin and eosin staining. The sham-operated group did not produce any detectable histomorphologic abnormalities. By contrast, the kidneys of $AChE^{+/+}$ I/R group mice (Fig. 3A) or vehicle-treated I/R rats (Fig. 3B) showed widespread degeneration of tubular architecture, tubular swelling, dilation, thinning, cellular vacuolization, pyknotic nuclei, medullary congestion and moderate to severe necrosis. Tubular injury (loss of proximal brush border, protein casts) was maximal in the area of the corticomedullary junction. Correspondingly, $AChE^{+/-}$ I/R group mice (Fig. 3A) or AChEI-treated I/R rats (Fig. 3B) exhibited a marked reduction of the histologic features of renal injury.

AChE deficiency or inhibition significantly attenuates renal dysfunction caused by I/R injury

Animals that underwent nephrectomized I/R exhibited a significant increase in the serum concentrations of creatinine and urea nitrogen as compared to sham-operated animals (Fig. 4), suggesting a significant degree of glomerular dysfunction. I/R induced deteriorative changes in renal functional parameters of $AChE^{+/-}$ mice were considerably small when compared with cases in $AChE^{+/+}$ mice (i.e. 200.8 ± 25.9 versus 121.5 ± 13.0 μmol/l serum creatinine and 36.1 ± 5.3 versus 23.8 ± 2.8 mmol/l for urea nitrogen,

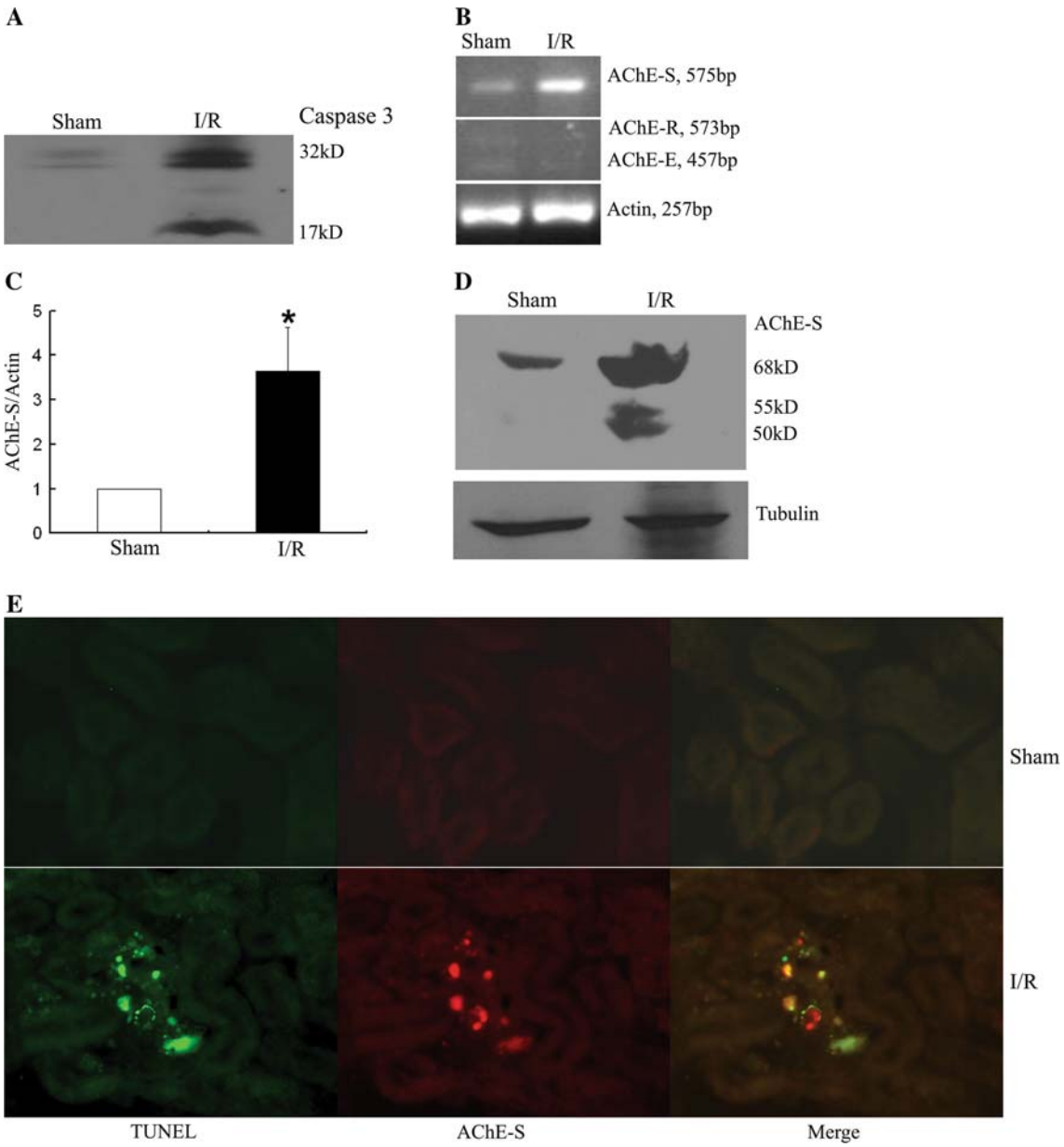

Fig. 2 Induction of AChE expression during apoptosis triggered by acute renal I/R injury in wild-type mice. **A** Caspase-3 protein expression in renal tissue cell lysates from sham and I/R groups. **B** Semi-quantitative RT–PCR of three different AChE isoforms mRNA in sham and I/R-treated renal tissue samples. **C** Real-time PCR of synaptic specific AChE mRNA in sham and I/R-treated renal tissue samples. **D** Western blot analysis of synaptic specific AChE protein in sham and I/R-treated renal tissue samples. **E** Co-localization of synaptic AChE and DNA fragmentation in apoptotic cells. TUNEL staining to detect DNA fragmentation (*green*) and immunofluorescence staining of AChE-S expression (*red*) were merged (*yellow*) for renal tissue sections of sham and I/R treated mice

respectively) (Fig. 4A, B). The administration of AChEIs also significantly reduced serum levels of creatinine and urea nitrogen compared to vehicle-treated rats. For example, levels of serum creatinine after treatment with I/R alone versus treatment with huperzine A, tacrine, or donepezil followed by I/R were 345.1 ± 64.0, 220.9 ± 53.2, 161.7 ± 54.6, and 173.3 ± 56.9 μmol/l, respectively. Levels of urea nitrogen after treatment with I/R alone versus treatment with huperzine A, tacrine, or donepezil followed by I/R were 61.6 ± 3.4, 51.8 ± 5.6, 28.9 ± 9.2, and 31.8 ± 6.8 mmol/l, respectively (Fig. 4C, D).

AChE deficiency or inhibition reduces tubular apoptosis caused by I/R injury

We investigated the abilities of AChE deficiency or inhibition to mediate protection against ischemia-induced apoptotic cell death. Animals were subjected to 90 min

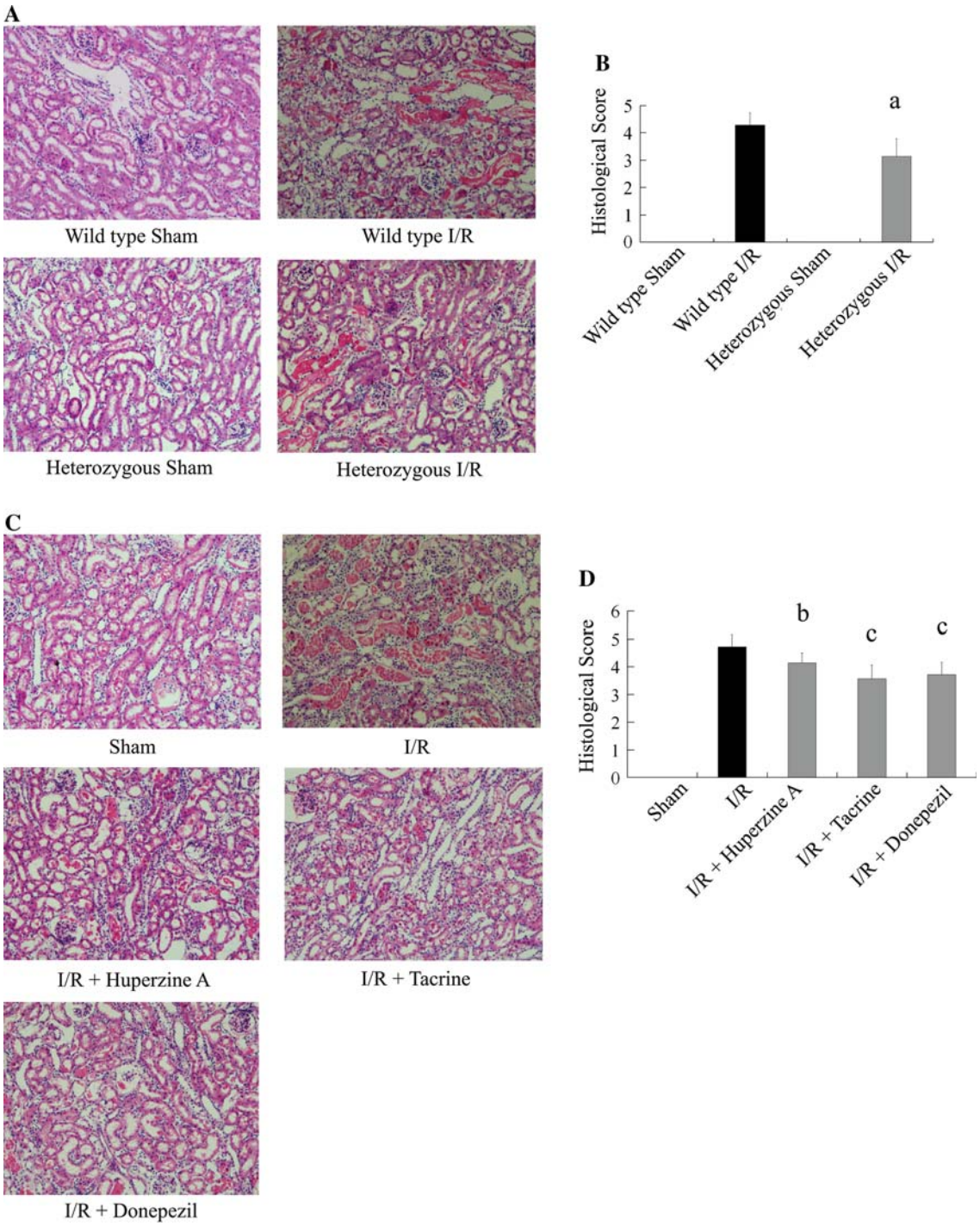

Fig. 3 AChE deficiency or inhibition attenuates the histomorphologic changes caused by I/R injury. **A** Kidney sections from the sham-operated and I/R-treated wild-type and $AChE^{+/-}$ mice stained with hematoxylin and eosin. **B** Quantitation by histological grading system. In the $AChE^{+/-}$ mice group the severity of injury decreased significantly. Data are expressed as mean ± SEM. [a] $P < 0.01$ compared with wild-type I/R. **C** Kidney sections from the sham-operated and ischemic groups of rats treated with AChEIs or vehicle stained with hematoxylin and eosin. **D** Quantitation by histological grading system. In the ischemic groups treated with AChEIs, the severity of injury decreased significantly. Data are expressed as mean ± SEM. [b] $P < 0.05$, [c] $P < 0.01$ compared with vehicle treated I/R group. Compared to wild-type mice or vehicle treated rats, sections from AChE deficiency or inhibition groups, tubules are largely intact with only focal sloughing of tubular cytoplasm and minimal loss of brush border

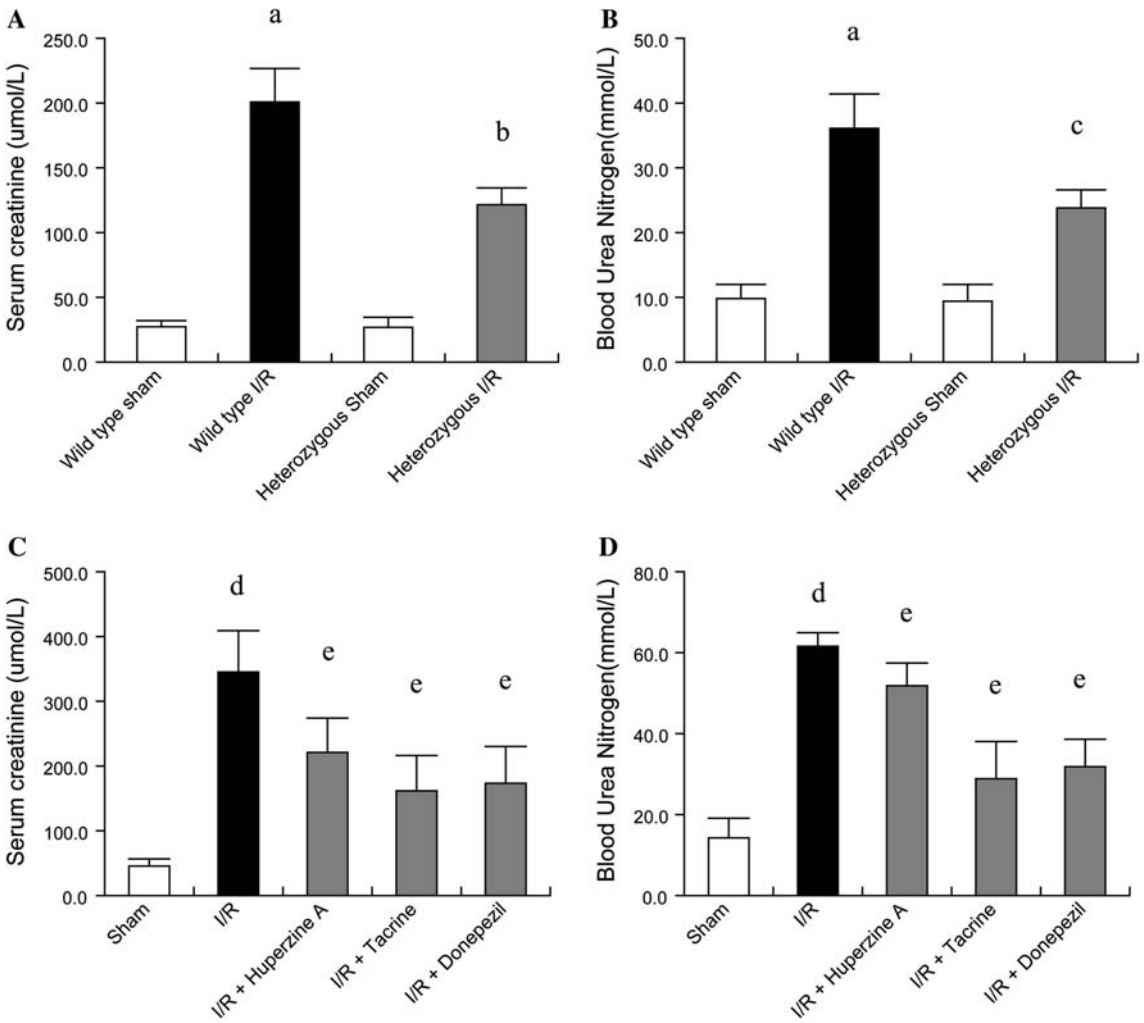

Fig. 4 Effect of AChE deficiency or inhibition on serum creatinine, and blood urea nitrogen (BUN) in animals exposed to renal I/R. **A** Levels of serum creatinine and **B** blood urea nitrogen were detected for sham-operated and I/R-treated wild-type and $AChE^{+/-}$ mice. Values are expressed as the means ± SEM. **C** Levels of serum creatinine and **D** blood urea nitrogen were detected for sham-treated rats, rats treated with I/R, and rats pre-treated with AChE chemical inhibitors prior to I/R treatment. Values are expressed as the means ± SEM. [a] $P < 0.01$ versus wild-type sham; [b] $P < 0.01$ versus wild-type I/R, [c] $P < 0.05$ versus wild-type I/R; $n = 4$–6. [d] $P < 0.01$ versus sham; [e] $P < 0.01$ versus vehicle treated I/R group; $n = 9$–10

ischemia followed by 24 h reperfusion. TUNEL staining was employed to evaluate apoptosis of renal tubular epithelial cells (Fig. 5). A significant number of TUNEL-positive cells were observed after I/R, predominantly located at the distal tubules of the outer medulla, fewer at the proximal tubules of the cortex. These cells demonstrated characteristic morphologies, e.g. condensed, pyknotic nuclei. In comparison, kidneys from sham-operated animals hardly had evidence of apoptosis and were negative for TUNEL staining. The number of TUNEL-positive nuclei was reduced significantly in heterozygous AChE deficient I/R group compared to WT I/R group (Fig. 5A). Likewise, administration of AChEIs before ischemia and after reperfusion significantly reduced the extent of apoptotic cell death compared to vehicle-treated group (Fig. 5B).

AChE deficiency or inhibition decreases caspases activation in I/R model

In humans and experimental models of renal ischemia, tubular cells in various nephron segments undergo apoptotic cell death accompanied by caspases activation [17].There was a marked increase in protein expression of active caspases-8, -9, -12 and caspase-3 in I/R kidneys compared to the sham-operated controls (Fig. 6). $AChE^{+/-}$ I/R group mice (Fig. 6A) or AChEIs-treated I/R rats (Fig. 6B) demonstrated an apparent reduction of the activation of caspases and reduced renal injury in contrast to the $AChE^{+/+}$ I/R group or vehicle-treated I/R rats respectively.

AChE protein expression in the kidneys of these animals was also examined. Western blot analysis demonstrated

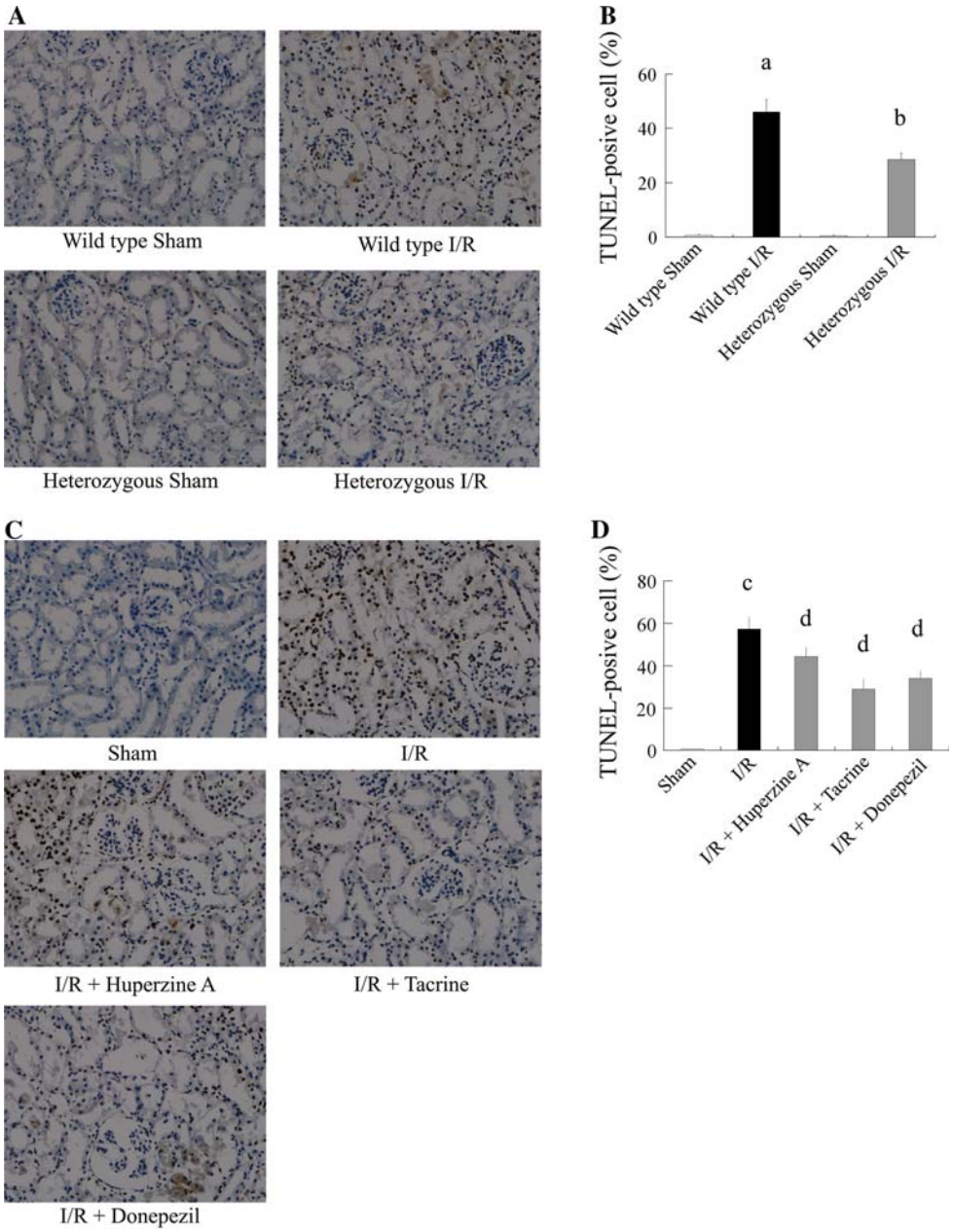

Fig. 5 AChE deficiency or inhibition reduces tubular apoptosis and necrotic cell death caused by I/R injury. Apoptosis was evaluated by TUNEL staining. **A** Kidney sections from the sham-operated and ischemic groups of wild-type and $ACHE^{+/-}$ mice. **B** Quantitative analyses of TUNEL-positive cells from the sham-operated and ischemic groups of wild-type and $ACHE^{+/-}$ mice. Data shown are mean ± SEM of four independent experiments. [a] $P < 0.01$ versus wild-type sham; [b] $P < 0.01$ versus wild-type I/R. **C** Kidney sections from the sham-operated and ischemic groups of rats treated with AChEIs or vehicle alone. **D** Quantitative analyses of TUNEL-positive cells from the sham-operated and ischemic groups of rats treated with AChEIs or vehicle alone. Data shown are mean ± SEM of four independent experiments. [c] $P < 0.01$ versus sham; [d] $P < 0.01$ versus vehicle treated I/R group

that the level of 68-kDa AChE-S protein expression in the AChE heterozygous mice was about half of that seen in wild-type mice either in sham or I/R renal tissues. Similarly, the apoptosis-specific 55/50-kDa AChE-S protein expression in the AChE heterozygous mice I/R renal tissues was also about half of that seen in wild-type mice (Fig. 6A). Compared with vehicle-treated I/R rats, AChEIs treatment had no obvious effect on the 68-kDa AChE-S protein expression but remarkably decreased the induction of the 55/50-kDa AChE-S protein isoform (Fig. 6B). These data demonstrated that the 55/50-kDa isoform has a positive correlation with apoptosis.

AChE deficiency attenuates I/R-induced over-expression of p53 and Bax and increases Bcl-2 protein expression

Previous studies have shown that the anti-apoptotic role of several AChEIs are related to alterations in p53, Bax and Bcl-2 proteins levels [5, 6], which are critical mediators of apoptotic signaling and regulate the activity of caspase proteins [18]. Our first series of experiments showed upregulated p53, Bax and Bcl-2 expression in I/R kidney compared with sham-operated controls. Interestingly, the upregulation of p53 and Bax could be reversed, while Bcl-2 protein expression was further increased by AChE

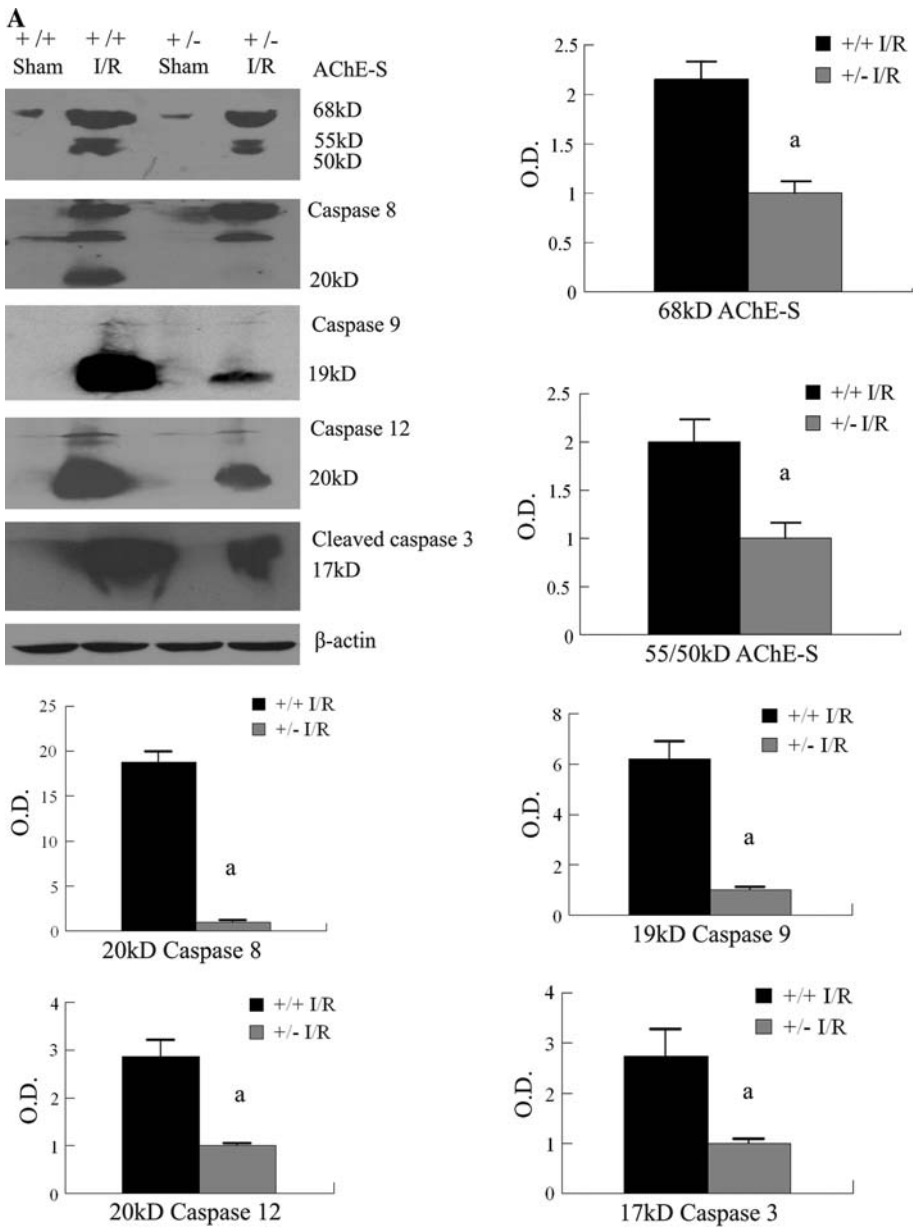

Fig. 6 AChE deficiency or inhibition decreases caspases activation in the I/R model. **A** Western blot analysis of AChE, caspase-8, caspase-9, caspase-12 and caspase-3 protein expression in the sham-operated and ischemic groups of wild-type and $AChE^{+/-}$ mice. **B** Western blot analysis of AChE, caspase-8, caspase-9, caspase-12 and caspase-3 protein expression in the sham-operated and ischemic groups of rats treated with vehicle or AChEIs. Results were representative of three experiments. Values are the means ± SEM ($n = 3$) and normalized by beta-actin and expressed as folds. [a] $P < 0.05$ versus wild-type I/R, [b] $P < 0.05$ versus vehicle treated I/R group

deficiency (Fig. 7). Subsequently we detected a change in p53 phosphorylation, which is an important regulatory mechanism for p53. I/R led to a significant increase in p53 phosphorylation at the serine-15 site as well as p53 induction. Such an increase was also ameliorated by AChE deficiency (Fig. 7A).

AChE activities were increased in I/R-treated renal tissues

A 1.8- to 1.9-fold increase in AChE activities were observed in I/R-treated renal tissues both in wild type and $AChE^{+/-}$ mice as compared to sham-operated animals. This observation is consistent with our previous findings [3]. The level of AChE activities in renal tissues of $AChE^{+/-}$ mice was approximately 70% of the level of AChE activities detected in both sham and I/R-operated wild type mice (Fig. 8A). Although AChE activities were significantly increased in I/R-treated renal tissues, the level of AChE activities in brain tissues were approximately 20-fold greater than the level in I/R-treated renal tissues of wild type and $AChE^{+/-}$ mice (Fig. 8B).

Discussion

Using AChE knockout mice in the present study, we directly demonstrated that AChE plays a pro-apoptotic role

Fig. 6 continued

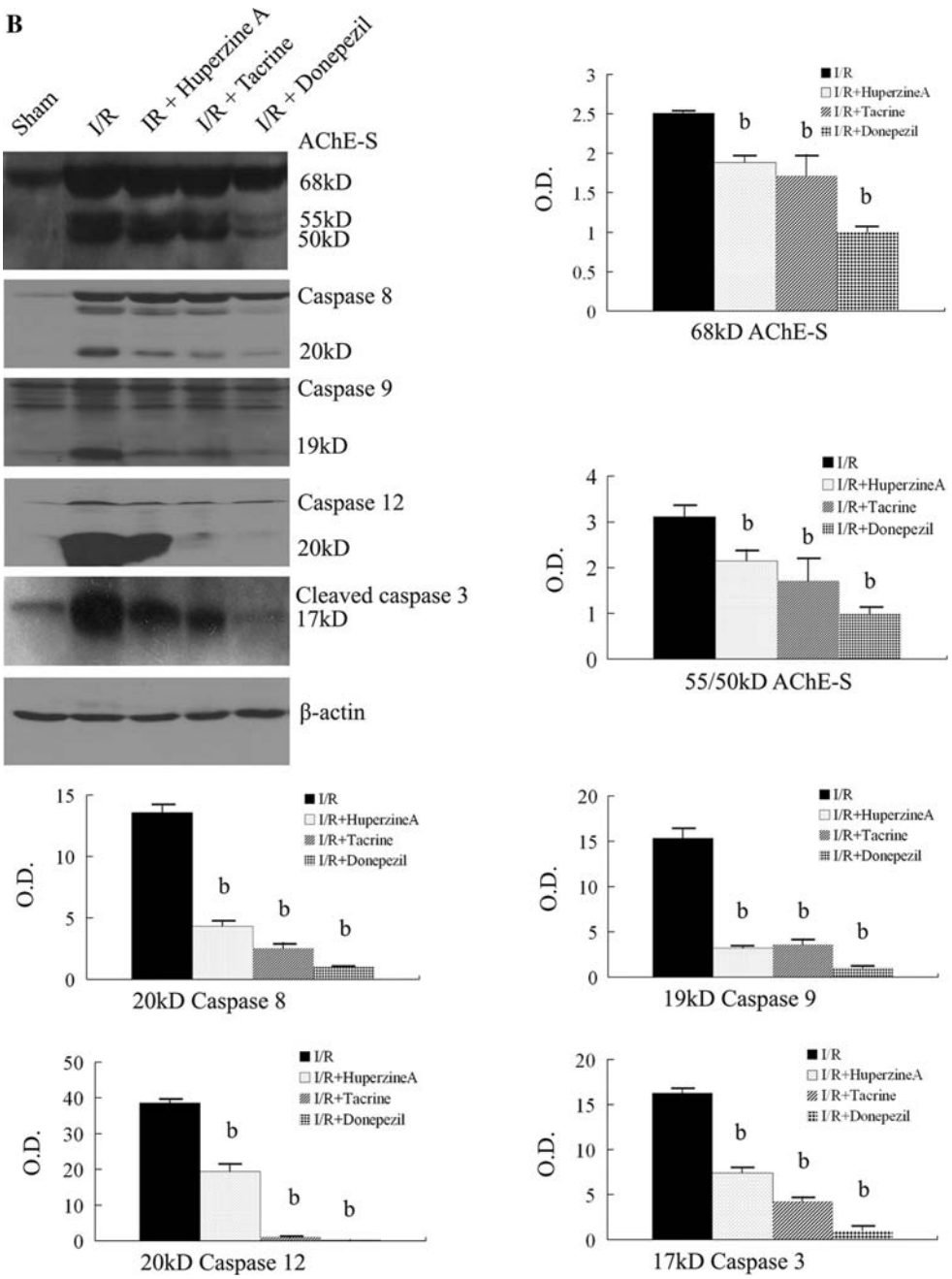

in vivo. I/R-induced renal dysfunction, histological damage and tubular apoptosis were alleviated in $AChE^{+/-}$ mice compared to cases in $AChE^{+/+}$ mice and to the pharmacological blockade of AChE with huperzine A, tacrine and donepezil. These results revealed the pathophysiological importance of AChE in I/R-induced apoptosis. Pitifully, $AChE^{-/-}$ mice have a high fetal mortality and are too feeble to undergo I/R-induced renal injury, and commonly die emaciated and dehydrated by 3 weeks of age. However, to more precisely elucidate the pathophysiological role of AChE, further studies using tissue-specific $AChE^{-/-}$ mice are essential.

Given the pro-apoptotic role associated with AChE in I/R injury model, we wished to further characterize the specific pathway involved in AChE-mediated apoptosis. Both AChE deficiency and AChE inhibition decreased the activation of caspases-8, -9, -12, and -3. Genetic evidence from knockout mice indicates that caspase-8 is required for all known death receptor-mediated apoptotic pathways, while caspase-9 is mostly involved in

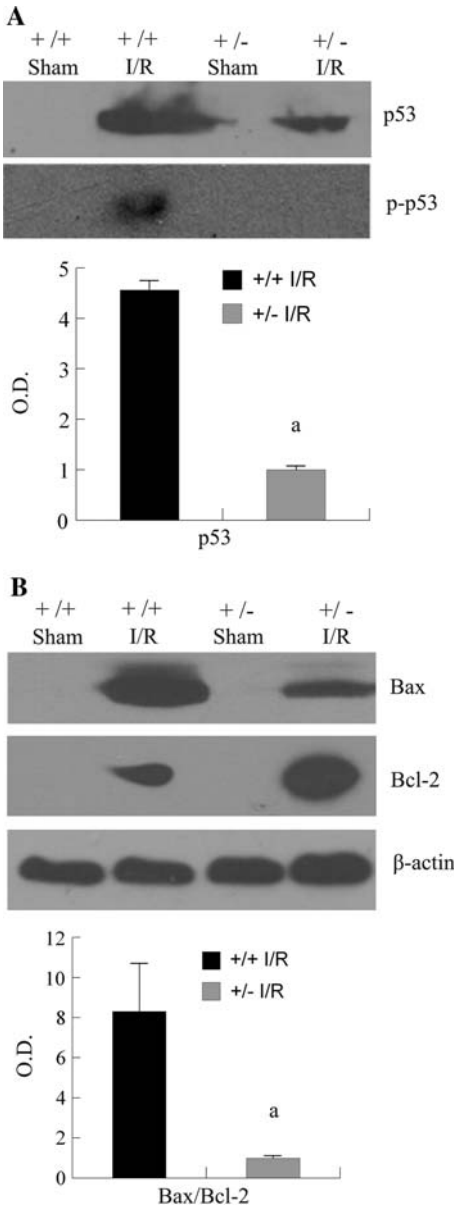

Fig. 7 AChE deficiency downregulates p53 induction and phosphorylation at serine-15 and decreases the Bax/Bcl-2 ratio during I/R. **A** Effect of AChE deficiency on p53 induction and phosphorylation at the site of serine-15 in ischemic ARF. **B** Effect of AChE deficiency on protein expression of Bax and Bcl-2 in ischemic ARF. Results were representative of three experiments. Values are the means ± SEM ($n = 3$) and normalized by beta-actin and expressed as folds. [a] $P < 0.01$ versus wild-type I/R

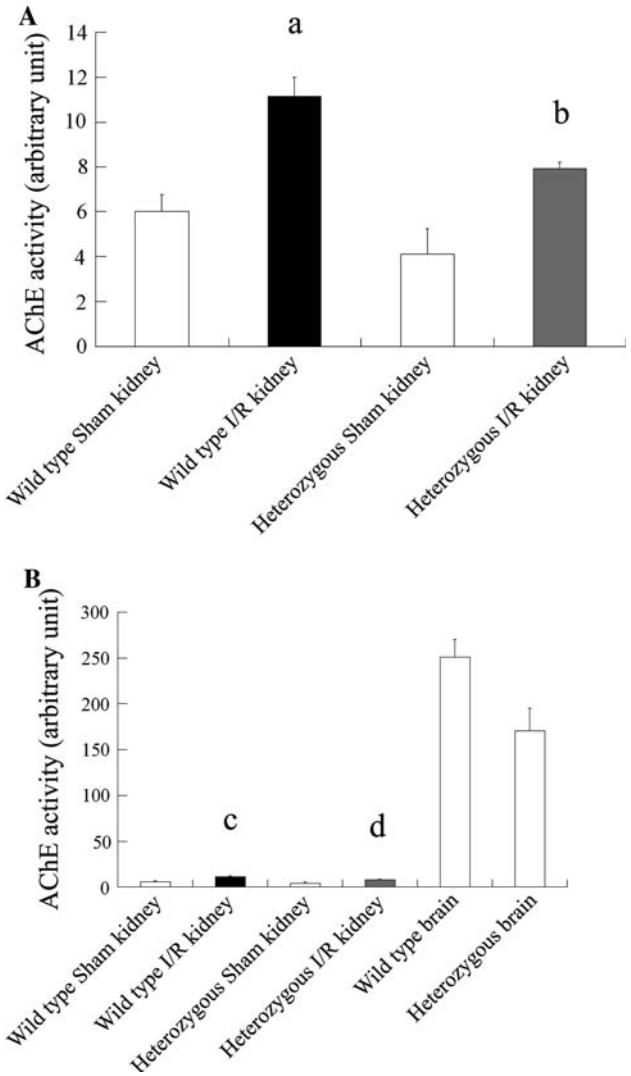

Fig. 8 **A** Up-regulation of AChE activities in I/R-treated renal tissues. The level of AChE activities in I/R-treated renal tissues of wild-type mice was approximately 1.5-fold more than that in $AChE^{+/-}$ mice. The densitometric graphs were presented as the means ± SEM of three separate experiments. [a] $P < 0.05$ versus wild-type sham; [b] $P < 0.05$ versus wild-type I/R. **B** The level of AChE activities in brain tissues were approximately 20-fold more than the level in I/R-treated renal tissues. The densitometric graphs were presented as the means ± SEM of three separate experiments. [c] $P < 0.01$ compared with wild-type brain tissues; [d] $P < 0.01$ compared with $AChE^{+/-}$ brain tissues. AChE activities were increased in I/R-treated renal tissues

mitochondria-mediated apoptotic pathways. Caspases-12 and -8 have both been implicated in endoplasmic reticulum stress-induced apoptosis [18–22], and caspase-3, a key factor in apoptosis execution, can be activated by caspases-8 and -9 [18].

In addition to the reduction of the activation of caspases-8, -9, -12 and -3, AChE deficiency downregulated the levels of both p53 induction and phosphorylation at the site of serine-15 and decreased the Bax/Bcl-2 ratio (Fig. 7). p53 is one of the crucial mediators of the two major apoptotic pathways, namely the extrinsic death receptor pathway and the intrinsic mitochondrial pathway [23, 24], and contributes to ER stress-induced apoptosis via activation of Puma and Noxa [25]. As a transcription factor, the tumor suppressor gene p53 has been reported to induce the upregulation of pro-apoptotic Bax and the downregulation of anti-apoptotic Bcl-2 [23, 26, 27]. An increase in the ratio

of Bax/Bcl-2 stimulates the release of cytochrome c from the mitochondria into the cytosol and the cytosolic cytochrome c then binds to Apaf-1, resulting in the activation of caspase-3 [28, 29]. p53 may also have nontranscriptional actions inactivating Bcl-2/Bcl-xL and activating Bax [23, 24, 26]. Intriguingly, p53 also boosts the activation of the caspase cascade by both transcription-dependent and -independent mechanisms [23]. Furthermore, p53 activity is modulated by various mechanisms and posttranscriptional phosphorylation and dephosphorylation may be key regulatory steps. p53 is phosphorylated on numerous serines in both the amino-and carboxy-terminal domains and phosphorylation of p53 at Ser15 leads to a reduced interaction between p53 and its negative regulator, MDM2. MDM2 inhibits p53 accumulation by targeting it for ubiquitination and proteasomal degradation [30]. Our experiments demonstrated a drastic decrease in p53 phosphorylation at Ser15 in AChE deficient I/R mice. Currently, the protein kinases or phosphatases involved in AChE deficiency that mediate the reduction of p53 phosphorylation remain to be identified.

However, the exact apoptotic pathways involved in the AChE-mediated apoptosis remain to be further elucidated. Our previous studies have revealed that intracellular calcium dyshomeostasis and cytosolic Ca^{2+} plays a key role in acetylcholinesterase regulation during apoptosis induced by two endoplasmic reticulum stess inducers, the calcium ionophore A23187 and the inhibitor of Ca^{2+}-ATPase thapsigargin [31]. We also show that activated calpain (a cytosolic calcium-activated cysteine protease), calcineurin (a calcium-dependent protein phosphatase) and GSK3β (an ubiquitous serine/threonine kinase activated by ER stress) [32] specifically regulate acetylcholinesterase expression during A23187- or thapsigargin induced apoptosis [16, 33] .

AChE expression is also mediated by the activation of JNK [34, 35], a key modulator in cell death mediated by reactive oxygen and nitrogen species and activated in response to different stimuli induced ER stress [21, 36, 37]. All of these studies strongly point to the AChE-S as an important regulator implicated in ER stress-mediated apoptotic execution.

Interestingly, AChE deficiency or inhibition not only decreases apoptotic cell death but also necrotic cell death. It appears that there is severe necrosis in I/R WT or vehicle-treated I/R animals but necrosis is attenuated in I/R $AChE^{+/-}$ or AChEIs-treated I/R groups. This finding may be due to the reduction of secondary necrosis. In vivo secondary necrosis occurs when massive apoptosis overwhelms the available scavenging capacity, or when the scavenger mechanism is directly impaired, and may result in leakage of the cell contents with induction of tissue injury [38].

Although the exact role of AChE-S in apoptotic process remains to be further investigated, AChE deficiency or inhibition appears to protect the kidney against I/R injury. We demonstrate that AChE deficiency or inhibition decreases caspases activation and prevents post-reperfusion tubular apoptotic cell death and improves the recovery of renal function. These results suggest that inhibition of AChE may represent a novel and valuable therapeutic approach for the prevention of I/R injury. The AChEIs used in our present study have already been approved as safe for the treatment of Alzheimer's disease in the clinical setting; therefore, their clinical application to kidney I/R injury may potentially be more readily accommodated than other compounds that do not have prior approved clinical applications.

Although the neuroprotective effects of several AChE inhibitors against apoptosis have been reported in vitro, these studies were limited to cell lines or primary cultured cells from the central or peripheral nervous system [5–12]. Explanations of the neuroprotective effect observed in these studies included activation of the central cholinergic system [10, 12], down-regulation of pro-apoptotic p53 and Bax, stimulation of anti-apoptotic Bcl-2 [5, 6, 9], or blockage of NMDA receptors [11]. However, no consideration of the role of AChE-S was proposed. Here we demonstrate that AChE-S itself plays a marked pro-apoptotic role in kidney I/R-induced apoptosis through the regulation of p53, Bax, and Bcl-2 proteins. While inhibition of AChE by three different AChEIs without cholinergic suppression decreased caspase activation and prevented tubular apoptotic cell death. Our finding regarding the proapoptotic effect of AChE-S provides further understanding of the loss of forebrain cholinergic neurons in the pathogenesis of AD and the therapeutic strategy for AD based on reversible inhibition of acetylcholinesterase. In other words, AChE-S induction and activation during apoptosis are likely to be importantly involved in the loss of cholinergic neurons in AD and might be influenced in a beneficial manner by AChEIs.

However, normal brain cholinergic neurons with high levels of AChE-S expression do not undergo apoptosis and AChE-S overexpression did not remarkably induce apoptosis in NRK cells. Instead, overexpression of AChE-S prevented NRK cell proliferation and promoted apoptosis upon serum deprivation [39], suggesting that AChE-S does not exhibit any toxic effects under normal growing conditions but has the potential to become pro-apoptotic once apoptosis is stimulated. An interesting apoptosis-specific 55/50-kDa AChE-S protein was detected by Western blot analysis (Figs. 2D, 6); therefore, it is highly possible that AChE-S functions via its 55/50-kDa isoform to promote apoptosis. Western blots of specific proteins fractionated using nuclear and cytoplasmic extraction reagents revealed

that the 68-kDa AChE-S protein is located the cytoplasm of living cells and in both the cytoplasm and nuclei of apoptotic cells, whereas the 55/50-kDa AChE-S predominately exists in the nuclei of apoptotic cells (data not shown). It is well known that proteolysis is a key regulatory process that promotes the activation, inactivation and translocation of proteins. The generation of active effector proteins such as caspases is a principal function of apoptotic proteolytic cascades. To identify whether the 55/50-kDa isoform of AChE-S may represent a proteolysis product of the 68-kDa isoform, mass spectrometry and N-terminal Edman sequencing would be needed. Additional studies are necessary to elucidate the role of the 55/50 kDa AChE-S isoform in apoptosis.

Also, the potential 68-kDa and 55/50-kDa AChE-S protein–protein interactions involved during apoptosis should be further investigated. A previous study showed that the interaction of CtBP and AChE-S competes with and impairs the formation of other CtBP complexes, which can interfere with CtBP's anti-apoptotic activities. This interaction may lay a molecular basis for the mechanism by which nuclear AChE-S induces a pro-apoptotic effect [40].

In conclusion, our present study demonstrates that AChE-S plays a pro-apoptotic role and regulates p53 and Bcl-2 family proteins expression during I/R-induced apoptosis. Inhibition of AChE-S may be useful in reducing I/R-induced apoptosis and enhancing the tolerance of the kidney against renal dysfunction and injury in situations where renal tissues may be subjected to periods of ischemia followed by reperfusion, e.g., during vascular surgery or renal transplantation. Our results also further elucidate the apoptotic mechanism of action as well as facilitate the development of therapeutic approaches that selectively target AChE expression pathways in the treatment of AD.

Acknowledgments This work was supported in part by grants from the Major State Basic Research Development Program of China (973 Program, No. 2007CB947901),the Third Phase Creative Program of Chinese Academy of Sciences (No. KSCX1-YW-R-13), the National Natural Science Foundation of China (Nos. 30971481 and 30623003).

References

1. Taylor P, Radic Z (1994) The cholinesterases: from genes to proteins. Annu Rev Pharmacol Toxicol 34:281–320
2. Soreq H, Seidman S (2001) Acetylcholinesterase–new roles for an old actor. Nat Rev Neurosci 2:294–302
3. Zhang XJ, Yang L, Zhao Q et al (2002) Induction of acetylcholinesterase expression during apoptosis in various cell types. Cell Death Differ 9:790–800
4. Toiber D, Berson A, Greenberg D, Melamed-Book N, Diamant S, Soreq H (2008) N-acetylcholinesterase-induced apoptosis in Alzheimer's disease. PLoS ONE 3:e3108
5. Wang R, Xiao XQ, Tang XC (2001) Huperzine A attenuates hydrogen peroxide-induced apoptosis by regulating expression of apoptosis-related genes in rat PC12 cells. Neuroreport 12:2629–2634
6. Wang R, Zhou J, Tang XC (2002) Tacrine attenuates hydrogen peroxide-induced apoptosis by regulating expression of apoptosis-related genes in rat PC12 cells. Brain Res Mol Brain Res 107:1–8
7. Gao X, Tang XC (2006) Huperzine A attenuates mitochondrial dysfunction in beta-amyloid-treated PC12 cells by reducing oxygen free radicals accumulation and improving mitochondrial energy metabolism. J Neurosci Res 83:1048–1057
8. Xiao XQ, Lee NT, Carlier PR, Pang Y, Han YF (2000) Bis(7)-tacrine, a promising anti-Alzheimer's agent, reduces hydrogen peroxide-induced injury in rat pheochromocytoma cells: comparison with tacrine. Neurosci Lett 290:197–200
9. Orozco C, de Los Rios C, Arias E et al (2004) ITH4012 (ethyl 5-amino-6, 7, 8, 9-tetrahydro-2-methyl-4-phenylbenzol[1, 8] naphthyridine-3-car boxylate), a novel acetylcholinesterase inhibitor with "calcium promotor" and neuroprotective properties. J Pharmacol Exp Ther 310:987–994
10. Takada Y, Yonezawa A, Kume T et al (2003) Nicotinic acetylcholine receptor-mediated neuroprotection by donepezil against glutamate neurotoxicity in rat cortical neurons. J Pharmacol Exp Ther 306:772–777
11. Li W, Pi R, Chan HH et al (2005) Novel dimeric acetylcholinesterase inhibitor bis7-tacrine, but not donepezil, prevents glutamate-induced neuronal apoptosis by blocking N-methyl-D-aspartate receptors. J Biol Chem 280:18179–18188
12. Zhao Y, Li W, Chow PC et al (2008) Bis(7)-tacrine, a promising anti-Alzheimer's dimer, affords dose- and time-dependent neuroprotection against transient focal cerebral ischemia. Neurosci Lett 439:160–164
13. Paulus JM, Maigne J, Keyhani E (1981) Mouse megakaryocytes secrete acetylcholinesterase. Blood 58:1100–1106
14. Roberts WL, Kim BH, Rosenberry TL (1987) Differences in the glycolipid membrane anchors of bovine and human erythrocyte acetylcholinesterases. Proc Natl Acad Sci USA 84:7817–7821
15. Su W, Wu J, Ye WY, Zhang XJ (2008) A monoclonal antibody against synaptic AChE: a useful tool for detecting apoptotic cells. Chem Biol Interact 175:101–107
16. Jing P, Jin Q, Wu J, Zhang XJ (2008) GSK3beta mediates the induced expression of synaptic acetylcholinesterase during apoptosis. J Neurochem 104:409–419
17. Padanilam BJ (2003) Cell death induced by acute renal injury: a perspective on the contributions of apoptosis and necrosis. Am J Physiol Renal Physiol 284:F608–627
18. Fan TJ, Han LH, Cong RS, Liang J (2005) Caspase family proteases and apoptosis. Acta Biochim Biophys Sin (Shanghai) 37:719–727
19. Rao RV, Ellerby HM, Bredesen DE (2004) Coupling endoplasmic reticulum stress to the cell death program. Cell Death Differ 11:372–380
20. Lamkanfi M, Kalai M, Vandenabeele P (2004) Caspase-12: an overview. Cell Death Differ 11:365–368
21. Momoi T (2004) Caspases involved in ER stress-mediated cell death. J Chem Neuroanat 28:101–105
22. Jimbo A, Fujita E, Kouroku Y et al (2003) ER stress induces caspase-8 activation, stimulating cytochrome c release and caspase-9 activation. Exp Cell Res 283:156–166
23. Haupt S, Berger M, Goldberg Z, Haupt Y (2003) Apoptosis—the p53 network. J Cell Sci 116:4077–4085
24. Moll UM, Wolff S, Speidel D, Deppert W (2005) Transcription-independent pro-apoptotic functions of p53. Curr Opin Cell Biol 17:631–636
25. Li J, Lee B, Lee AS (2006) Endoplasmic reticulum stress-induced apoptosis: multiple pathways and activation of p53-up-regulated modulator of apoptosis (PUMA) and NOXA by p53. J Biol Chem 281:7260–7270

26. Levine AJ, Hu W, Feng Z (2006) The P53 pathway: what questions remain to be explored? Cell Death Differ 13:1027–1036
27. Chipuk JE, Green DR (2006) Dissecting p53-dependent apoptosis. Cell Death Differ 13:994–1002
28. Pandey P, Saleh A, Nakazawa A et al (2000) Negative regulation of cytochrome c-mediated oligomerization of Apaf-1 and activation of procaspase-9 by heat shock protein 90. EMBO J 19: 4310–4322
29. Bossy-Wetzel E, Green DR (1999) Caspases induce cytochrome c release from mitochondria by activating cytosolic factors. J Biol Chem 274:17484–17490
30. Shieh SY, Ikeda M, Taya Y, Prives C (1997) DNA damage-induced phosphorylation of p53 alleviates inhibition by MDM2. Cell 91:325–334
31. Zhu H, Gao W, Jiang H et al (2007) Regulation of acetylcholinesterase expression by calcium signaling during calcium ionophore A23187- and thapsigargin-induced apoptosis. Int J Biochem Cell Biol 39:93–108
32. Song L, De Sarno P, Jope RS (2002) Central role of glycogen synthase kinase-3beta in endoplasmic reticulum stress-induced caspase-3 activation. J Biol Chem 277:44701–44708
33. Zhu H, Gao W, Jiang H, Wu J, Shi YF, Zhang XJ (2007) Calcineurin mediates acetylcholinesterase expression during calcium ionophore A23187-induced HeLa cell apoptosis. Biochim Biophys Acta 1773:593–602
34. Deng R, Li W, Guan Z et al (2006) Acetylcholinesterase expression mediated by c-Jun-NH2-terminal kinase pathway during anticancer drug-induced apoptosis. Oncogene 25:7070–7077
35. Zhang JY, Jiang H, Gao W et al (2008) The JNK/AP1/ATF2 pathway is involved in H2O2-induced acetylcholinesterase expression during apoptosis. Cell Mol Life Sci 65:1435–1445
36. Shen HM, Liu ZG (2006) JNK signaling pathway is a key modulator in cell death mediated by reactive oxygen and nitrogen species. Free Radic Biol Med 40:928–939
37. Urano F, Wang X, Bertolotti A et al (2000) Coupling of stress in the ER to activation of JNK protein kinases by transmembrane protein kinase IRE1. Science 287:664–666
38. Silva MT, do Vale A, dos Santos NM (2008) Secondary necrosis in multicellular animals: an outcome of apoptosis with pathogenic implications. Apoptosis 13:463–482
39. Jin QH, He HY, Shi YF, Lu H, Zhang XJ (2004) Overexpression of acetylcholinesterase inhibited cell proliferation and promoted apoptosis in NRK cells. Acta Pharmacol Sin 25:1013–1021
40. Perry C, Pick M, Podoly E et al (2007) Acetylcholinesterase/C terminal binding protein interactions modify Ikaros functions, causing T lymphopenia. Leukemia 21:1472–1480